



Development of bulk heterojunction morphology by the difference of intermolecular interaction behaviors

Hyojung Cha^a, Jang Yeol Baek^b, Tae Kyu An^a, Seul-Ong Kim^b, Soon-Ki Kwon^{b,*}, Yun-Hi Kim^{c,*}, Chan Eon Park^{a,*}

^a Department of Chemical Engineering, Pohang University of Science and Technology (POSTECH), Pohang 790-784, Republic of Korea

^b School of Materials Science & Engineering, Engineering Research Institute (ERI), Gyeongsang National University, Jinju 660-701, Republic of Korea

^c Department of Chemistry, Engineering Research Institute (ERI), Gyeongsang National University, Jinju 660-701, Republic of Korea

ARTICLE INFO

Article history:

Received 7 July 2014

Received in revised form 3 October 2014

Accepted 3 October 2014

Available online 18 October 2014

Keywords:

Bulk heterojunction morphology

Processing additive

Phase separation

Electronegativity

Crystallinity

ABSTRACT

The morphology of a bulk heterojunction can be controlled by adding a processing additive in order to improve its power conversion efficiency (PCE) in photovoltaic devices. The phase-separated morphologies of blends of **PONTBT** or **P3HT** with fullerene derivatives are systematically examined in the presence of processing additives that possess various alkane alkyl chain lengths or end-group electronegativities. We determined the morphologies of the bulk heterojunction layers by using atomic force microscopy (AFM) and grazing incidence wide angle X-ray scattering (GIWAXS). The photocurrent–voltage characteristics of the bulk heterojunction solar cells were found to be strongly dependent on the intermolecular interactions between the conjugated polymers, the fullerene derivatives, and the processing additives in the photoactive layer. The optimal **PONTBT**:fullerene derivative blend morphology was obtained with a processing additive, 1,3-diiodopropane (1,3-DIP), that possesses a short alkyl chain and an end group with weak electronegativity, and was found to exhibit a high fill factor (FF) and a high current density (J_{sc}). In contrast, in blends of **P3HT** with the fullerene derivative, PCEs with higher FF and J_{sc} values were achieved by incorporating the processing additive, 1,8-dibromooctane (1,8-DBrO), which has a long alkyl chain and a strong electronegative end group. Thus the selection of the processing additive with the aim of enhancing photovoltaic performance needs to take into account the intermolecular interaction of the conjugated polymer.

© 2014 Elsevier B.V. All rights reserved.

1. Introduction

Over the last few years, high power conversion efficiencies (PCEs) have been achieved in bulk heterojunction solar cells with bi-continuous interpenetrating donor:acceptor (D:A) networks; in some recent studies, PCEs approaching 10% have even been reported [1–10]. In addition to the intrinsic properties of the active layer, the morphological

properties of the D:A blend including the crystallinity of the polymers [11–13], domain size [14–16], miscibility of the component materials [17], and molecular orientation [18] are also important for the photovoltaic performance of a given device. Several strategies, including slow growth [19], solvent annealing [20,21], thermal annealing [22,23], and selection of the solvent [24–29] or mixed solvent [30,31], have been tested in the control of the morphology of D:A blends. In particular, binary solvent mixtures containing poor solvents for the conjugated polymers have been successfully used in morphology control [32–42]. For example, dichlorobenzene (DCB) or chlorobenzene

* Corresponding authors.

E-mail addresses: skwon@gnu.ac.kr (S.-K. Kwon), ykim@gnu.ac.kr (Y.-H. Kim), cep@postech.ac.kr (C.E. Park).

(CB):1,8-diiodooctane (1,8-DIO) binary solvent systems have been widely applied in organic photovoltaic device (OPV) fabrication processes. By mixing a few volume percent of processing additives with the host solvent (DCB or CB), the efficiencies of many polymer-based solar cells can be improved dramatically [32–38]. The advantage of the processing additive approach is that a phase-separated morphology develops in the bulk heterojunction layer through the use of a single-step spin-coating process without post treatment [39,40]. According to these studies, the crystallinity of the polymers and the domain sizes in D:A blends can be tuned effectively by using binary solvent mixtures, and thus binary solvent mixtures play a very important role in the fabrication of high performance OPVs [32–34].

Peet et al. showed that processing additives can be introduced into D:A blends to control domain sizes and thus maximize charge generation and collection in bulk heterojunction layers, which increases the efficiency of organic photovoltaic devices [32,33]. Lee et al. concluded that processing additives require good miscibility with the host solvent, a higher boiling point than the host solvent, and a good solubility with respect to the fullerene derivative, and that these properties enable control of phase separation [34]. Furthermore, the effects on photovoltaic device performance of a few other processing additives, such as several alkanedithiols with various alkane chain lengths or electronegative end groups [33,34,39,40], N-methyl-2-pyrrolidinone [41], and 4-bromoanisole [42], have been investigated. Despite this increasing interest in processing additives, few studies have investigated how the intrinsic intermolecular interaction of the conjugate polymer needs to be taken into account in the selection of such processing additives.

In this study, we investigated the effects of the intermolecular interactions of the conjugated polymers in bulk heterojunction active layers on their phase-separation behavior by selecting two conjugated polymers with different crystallinities, and testing the responses of their blends with fullerene derivatives to the incorporation of various processing additives. We synthesized a new alkoxy naphthalene-based amorphous polymer, poly(4-(5-(1,5-bis(octyloxy)naphthalen-2-yl)thiophen-2-yl)-7-(thiophen-2-yl)benzo[c][1,2,5]thiadiazole) (**PONTBT**) (Fig. 1). Previously, we have reported an alkoxy naphthalene-based conjugated polymer that exhibits amorphous behavior and a high PCE of 4.2% in a bulk heterojunction active layer upon mixing with [6,6]-phenyl-C71-butyric acid methyl

ester (PC₇₁BM) [43]. **PONTBT** has an octyl side chain to modify its energy levels and its UV-visible absorption spectrum with respect to those of previous alkoxy naphthalene-based conjugated polymers. Blends of **PONTBT**, or poly(3-hexylthiophene-2,5-diyl) (**P3HT**), respectively, with fullerene derivatives and various processing additives with various alkyl chain lengths and end-group electronegativities were systematically examined [43–45]. The interpenetrating network morphologies of the bulk heterojunction layers were determined with atomic force microscopy (AFM) and grazing incidence wide angle X-ray scattering (GIWAXS). The photovoltaic device performances were found to be strongly dependent on the selection of the processing additive and the intrinsic intermolecular interaction of the conjugated polymer. The effects of processing additives on the blends containing highly crystalline **P3HT** are not as significant as in the case of **PONTBT**. In other words, the introduction of processing additives into **PONTBT**:PC₇₁BM is more effective than for **P3HT**:PC₆₁BM.

2. Material and methods

Organic solar cells were fabricated with the structure ITO/PEDOT:PSS/conjugated polymer and fullerene derivative blend/LiF/Al. A glass substrate with a pre-patterned ITO active layer with a thickness of 0.09 mm² was ultrasonicated in detergent, D.I. water, CMOS-grade acetone, and isopropanol, and the surface of the glass substrate was modified with UV-ozone treatment for 20 min. PEDOT:PSS (Bay P VP AI4083, Bayer AG) for hole injection was spin-coated at 4000 rpm for 60 s for a thickness of 30–40 nm, as measured with an alpha-stepper, on the cleaned ITO-patterned glass substrate after filtration through a 0.45 μm filter, followed by baking in an oven at 120 °C for more than an hour.

The organic solar cells consisted of a conjugated polymer as the electron donor and a fullerene derivative as the electron acceptor. The conjugated polymer, **PONTBT**, was synthesized via a palladium-catalyzed Stille coupling reaction, as described in the supporting information. The molecular weight of **PONTBT** was 16 kDa. The electron donor conjugated polymer, **P3HT**, was obtained from Rieke Metals. The PC₆₁BM and PC₇₁BM fullerene derivatives (99.5%) were obtained from Nano-C. Solutions of the conjugated polymer/fullerene derivative with 2 vol% of a processing additive were prepared in dichlorobenzene to

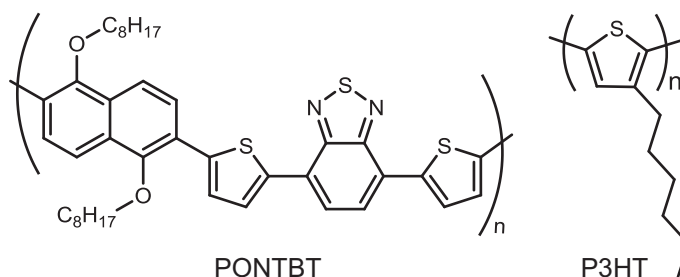


Fig. 1. Structures of the amorphous polymer **PONTBT** and the highly ordered crystalline polymer **P3HT**.

yield 40 mg/mL solutions that were stirred in a glove box under a nitrogen atmosphere overnight. The blended solutions were spin-coated at 1000 rpm for 60 s for a thickness of 100 nm on top of the PEDOT:PSS layer after filtration with a 0.2 μm PTFE filter for all solvents, then annealed at various temperatures for 20 min on a hot plate in the glove box. In all the devices, the **PONTBT**:PC₇₁BM layers had similar thicknesses, on the order of 100 nm, and the **P3HT**:PC₆₁BM layers had similar thicknesses of 120 nm, as measured with an alpha-stepper. LiF and Al cathodes were thermally deposited to thicknesses of 1 and 100 nm respectively onto the surface of each active layer.

The J - V characteristics were measured by using a Keithley 4200 source measurement unit in the dark and under AM 1.5G solar illumination (Oriel 1 kW solar simulator) with respect to a reference cell PVM 132 calibrated at the National Renewable Energy Laboratory at an intensity of 100 mW/cm².

UV-visible (Cary, Varian Co.) and PL (FR 650, JASCO Co.) measurements were used to analyze the optical properties of the conjugated polymer/fullerene derivative blends. AFM (Multimode IIIa, Digital Instruments) was performed in tapping mode to acquire images of the surfaces of the conjugated polymer/fullerene derivative blend films. In the transmission electron microscopy (TEM) measurements, the conjugated polymer/fullerene derivative layers on a water-soluble PEDOT:PSS substrate were floated on the surface of deionized water and picked up using 200-mesh copper TEM grids. TEM images were obtained by using a HITACHI-7600 operated at 100 kV. GIWAXS data were obtained at the 5A beamline ($E = 11.57$ keV) of the Pohang Accelerator Laboratory (PAL) [46]. Total external reflection angle of GIWAXS measurements is 0.14° to unify the penetration depth of thin films. 6 Circle diffractometer and scintillation detector are used to control external reflection angle with no calibration standard. The exposure time was 1 s at each measured angles.

3. Results and discussion

3.1. Properties of **PONTBT** and the optimization of the **PONTBT**:PC₇₁BM Solar Cells

The amorphous polymer, **PONTBT**, was synthesized with the procedures shown in **Scheme S1** and described in the [supporting information](#). The number average molecular weight (M_n) of **PONTBT** is 16.2 kDa. The resulting copolymer is soluble in toluene, chloroform, CB, and DCB. The thermal properties of **PONTBT** were investigated with thermogravimetric analysis (TGA) and differential scanning calorimetry (DSC), as shown in **Fig. S1**. This molecule exhibits excellent thermal stability: the decomposition temperature for 5% weight loss is approx. 344 °C. The DSC traces for this compound contain a peak indicative of phase transitions at 222 °C.

The electrochemical and optical properties of **PONTBT** were determined in order to optimize the **PONTBT**:PC₇₁BM blend solar cells. **Fig. S2** shows the UV-visible absorption spectra of **PONTBT** in chloroform solution and in the film state and the cyclic voltammogram for **PONTBT**. Our

electrochemical analysis showed that the highest occupied molecular orbital (HOMO) energy level of **PONTBT** is -5.34 eV, the lowest unoccupied molecular orbital (LUMO) energy level of **PONTBT** is -3.60 eV, and its band gap is 1.74 eV. **Table S1** provides a summary of the electrochemical and electrical properties of **PONTBT**. The spectrum of the **PONTBT** film contains a high energy absorption maximum at 595 nm, which indicates that **PONTBT** is a low band gap polymer. Structural analysis with atomic force microscopy (AFM), transmission electron microscopy (TEM), and grazing incidence wide angle X-ray scattering (GIWAXS) was performed to determine the molecular ordering and the film morphologies of **PONTBT** and **PONTBT**:PC₇₁BM. The films were prepared by dissolving **PONTBT** and **PONTBT**:PC₇₁BM in DCB, followed by spin-coating at 1000 rpm onto ITO glass coated with PEDOT:PSS. An AFM image of a **PONTBT** film is shown in **Fig. S3(a)**. The **PONTBT** film has an r.m.s. roughness of 0.459 nm. The bulk morphology of the **PONTBT**:PC₇₁BM film was analyzed with TEM. **Fig. S3(b)** shows a TEM image of a homogeneous **PONTBT**:PC₇₁BM domain. The dark areas are attributed to PCBM-rich regions because their electron scattering density is higher than that of the polymer. **Fig. S3(c)** shows GIWAXS patterns of **PONTBT** and **PONTBT**:PC₇₁BM films. Neither GIWAXS pattern contains any Bragg reflection peak, which confirms that both films are amorphous.

The measured current-voltage (J - V) curves in **Fig. S4** shows that the device performance is strongly dependent on the ratio of **PONTBT** and PC₇₁BM. The photovoltaic results for all of the investigated blends under illumination with an intensity of 100 mW cm⁻² are summarized in **Table S2**. The device with a 1:3 weight ratio of conjugated polymer to PC₇₁BM was found to exhibit the best PCE.

3.2. Optical properties of the conjugated polymer/fullerene derivative blends with various processing additives

Solar cell performance can be optimized by the addition of processing additives to the conjugated polymer/fullerene derivative blend layers. The conjugated polymer/fullerene derivative ratios were optimized at 1:3 (wt:wt) for **PONTBT**:PC₇₁BM in DCB and 1:1 (wt:wt) for **P3HT**:PC₆₁BM in CB. In this study, processing additives with various alkyl chain lengths and end-group electronegativities were incorporated into these optimized blends.

As shown in **Fig. 2**, the absorption maximum of the **PONTBT**:PC₇₁BM blends is at 550 nm. When 2 vol% of the additives are added to the host solvent, DCB, the absorption intensity in the region 600–700 nm increases, which is indicative of the close packing of **PONTBT** and a red-shift in the π - π absorption band. The intensities of the intermolecular interactions of **PONTBT** are increased by the addition of the processing additives. Moreover, the intensities of the shoulders at 650 nm in the spectra of the **PONTBT**:PC₇₁BM blends increase with increases in the alkyl chain length (**Fig. 2(a)**) and in the electronegativity ($\text{Cl} > \text{Br} > \text{I}$) of the end group (**Fig. 2(b)**) of the processing additives. The incorporation of the processing additives into the **PONTBT**:PC₇₁BM (1:3, w/w) blend results in the close packing of **PONTBT** and better phase separation of **PONTBT** and the fullerene derivative.

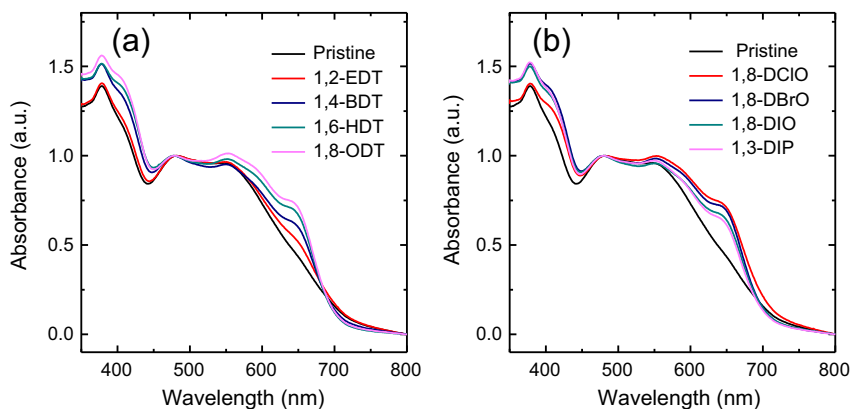


Fig. 2. UV-visible spectra of **PONTBT**:**PC**₇₁**BM** (1:3, w/w) films cast from dichlorobenzene (DCB) and **PONTBT**:**PC**₇₁**BM** (1:3, w/w) films cast from DCB containing 2% of the processing additives with (a) various alkyl chain lengths and (b) end groups with various electronegativities.

Similarly, by adding 2 vol% of the processing additives into the **P3HT**:**PC**₆₁**BM** (1:1, w/w) blend solutions, the intensity of the absorption increases in the region 600–700 nm (Fig. 3). The peaks in the absorption bands of **P3HT** in the **P3HT**:**PC**₆₁**BM** blends with processing additives are red-shifted by 12 nm and have a stronger red shoulder (600 nm) than annealed **P3HT**:**PC**₆₁**BM** without any processing additive. The absorption maxima of the annealed **P3HT**:**PC**₆₁**BM** film and the 1,9-NDT-treated **P3HT**:**PC**₆₁**BM** film are at 507 nm and 519 nm respectively. The additions of processing additives to the **PONTBT**:**PC**₇₁**BM** and **P3HT**:**PC**₆₁**BM** blend films increase the strengths of the intermolecular interactions between the conjugated polymers, the fullerene derivatives, and the processing additives.

3.3. Morphologies of the conjugated polymer/fullerene derivative blends with various processing additives

The morphologies of the blends with and without the processing additives were investigated by using GIWAXS and AFM. The GIWAXS patterns for the **PONTBT**:**PC**₇₁**BM** blends containing the additives 1,3-propanedithiol

(1,3-PDT), 1,8-diiodooctane (1,8-DIO), and 1,3-diiodopropane (1,3-DIP) do not contain Bragg reflection peaks because **PONTBT** is an amorphous polymer (Fig. S5). For **P3HT**:**PC**₆₁**BM**, Bragg scattering signals due to the π - π spacing (approximately 4 Å) and the lamella spacing (approximately 20 Å) in the conjugated polymer film are present, as well as the higher order reflections of crystalline films. The intensity of the first Bragg reflection peak for thin films of **P3HT**:**PC**₆₁**BM** containing various processing additives varies with the additive (Fig. 4). A comparison of the d-spacings in the six systems (Fig. 4(a) and (b)) clearly shows that the addition of processing additives with longer alkyl chains produces blends with shorter d-spacings than the addition of additives with shorter alkyl chains. The **P3HT** crystallites in **P3HT**:**PC**₆₁**BM** are oriented in the (100) plane, in the so-called ‘edge-on’ orientation. The as-cast **P3HT**:**PC**₆₁**BM** blend layer without processing additives has a d-spacing of 1.83 nm at 3.36°, whereas the **P3HT**:**PC**₆₁**BM** blend layer with 1,9-nonanedithiol (1,9-NDT) has a d-spacing of 1.58 nm at 3.88° (Fig. 4(b)). The d-spacings of the **P3HT**:**PC**₆₁**BM** blend layers with processing additives with longer alkyl chains are clearly less than those of the **P3HT**:**PC**₆₁**BM** blends with additives with

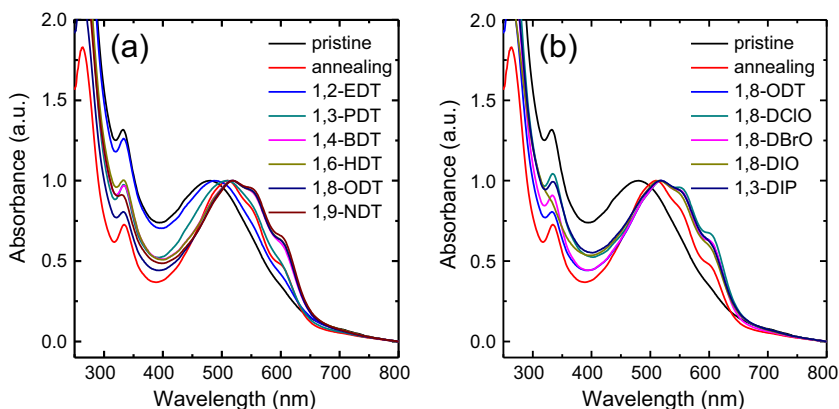


Fig. 3. UV-visible spectra of **P3HT**:**PC**₆₁**BM** (1:1, w/w) films cast from chlorobenzene (CB) and **P3HT**:**PC**₆₁**BM** (1:1, w/w) films cast from CB containing 2% of the processing additives with (a) various alkyl chain lengths and (b) end groups with various electronegativities.

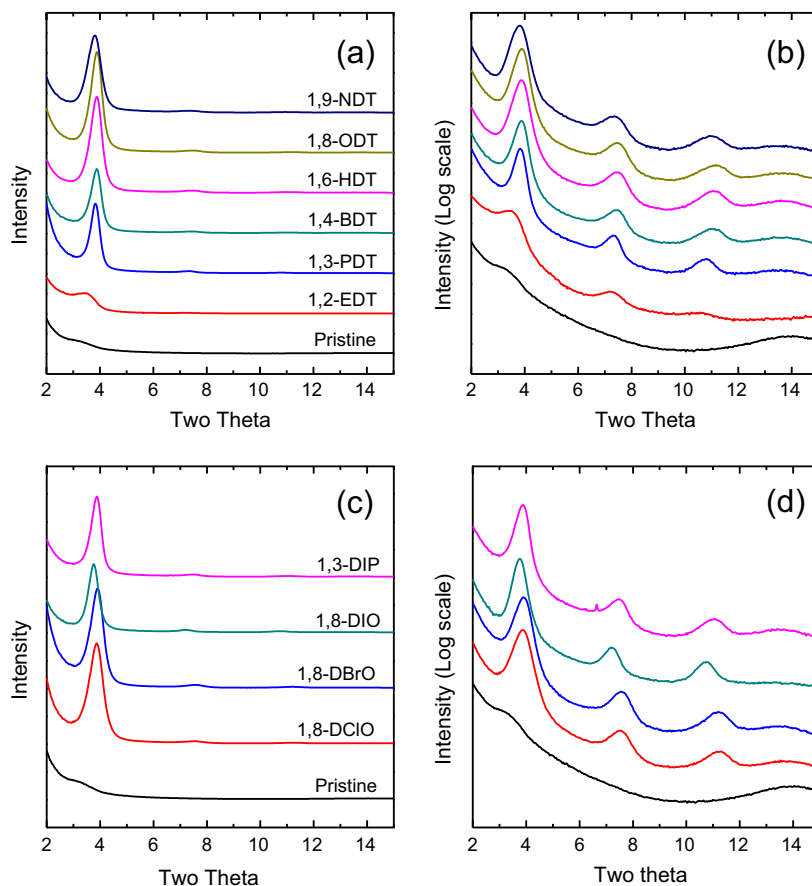


Fig. 4. One-dimensional GIWAXS patterns for a **P3HT**:**PC₆₁BM** blend film without any processing additive and for **P3HT**:**PC₆₁BM** blend films cast from chlorobenzene (CB) containing 2% of the processing additives with various alkyl chain lengths (a) on a linear scale and (b) on a log scale, and 2% of the processing additives with end groups with various electronegativities (c) on a linear scale and (d) on a log scale.

shorter alkyl chains. Similarly, the comparison of the d-spacings of the blends with processing additives with end groups of three different electronegativities (Fig. 4(c) and (d)) shows that the incorporation of additives with end groups that have higher electronegativities results in larger d-spacings than the incorporation of an additive with an end group with a lower electronegativity.

Fig. 5 shows typical AFM height images of the blend films processed with additives with various alkyl chain lengths (the image size is $5\ \mu\text{m} \times 5\ \mu\text{m}$). As the alkyl chain lengths of the processing additives in the **PONTBT**:**PC₇₁BM** blends increase from that of 1,2-ethanedithiol (1,2-EDT) to that of 1,9-NDT, the films contain more connected blend networks and larger domains, and the top surfaces become rougher. As the electronegativities of the end groups of the processing additives in the **PONTBT**:**PC₇₁BM** blend layers increase from that of 1,8-DIO to that of 1,8-dichlorooctane (1,8-DCIO), the phase separation is enhanced. Although **PONTBT**:**PC₇₁BM** is smooth in the AFM image in Fig. 5, the addition of processing additives significantly modifies its surface topography. Since **PC₇₁BM** is soluble in the processing additives, the phase separation of **PONTBT** and **PC₇₁BM** is increased. Decreasing the alkyl chain length and reducing the electronegativity of the end group of the processing additives increases the phase separation of

the conjugated polymer and the fullerene derivative, which enhances carrier transport [20].

The r.m.s. roughnesses of **P3HT**:**PC₆₁BM** blends with processing additives with longer alkyl chains or end groups with stronger electronegativities (Fig. 6) are not significantly higher than those of the **PONTBT**:**PC₇₁BM** blends (Fig. 5) because the intermolecular interactions of **P3HT** and fullerene derivatives are stronger than those between **PONTBT** and fullerene derivatives. The intermolecular interactions between **PONTBT**:**PC₇₁BM** and the processing additives induce the phase separation of **PONTBT** and **PC₇₁BM**. In other words, **PC₇₁BM** molecules, which are selectively dissolved by the processing additives, increase the aggregation of **PONTBT**.

3.4. Photovoltaic performances of the conjugated polymer/fullerene derivative blends with processing additives

The photovoltaic properties of the conjugated polymer/fullerene derivative blends incorporating processing additives were investigated in bulk heterojunction solar cells with the configuration glass/ITO/PEDOT:PSS/active layer/LiF/Al.

Fig. S6 presents the *J*-*V* curves for devices prepared from **PONTBT**:**PC₇₁BM** blends with various processing additives.

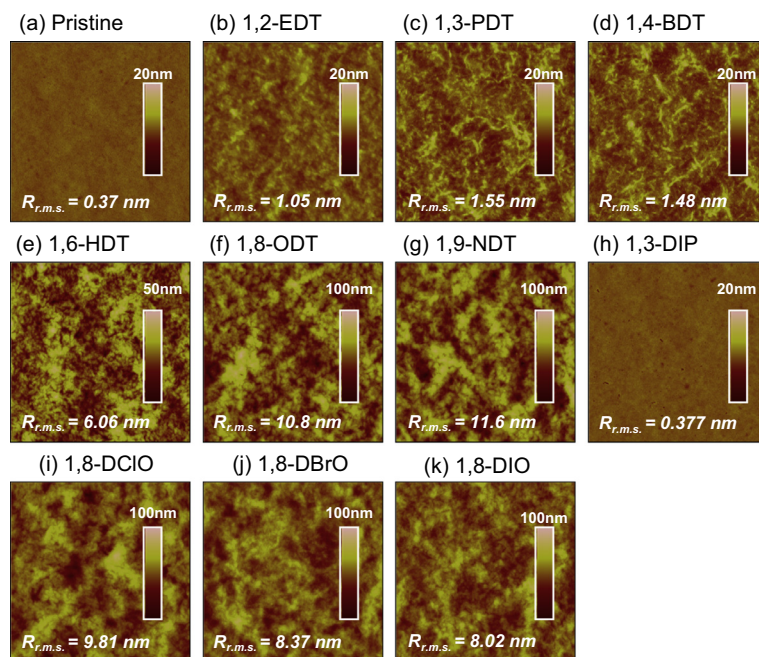


Fig. 5. AFM topographies of films cast from **PONTBT:PC₇₁BM**: (a) without additives; with the additives (b) 1,2-ethanedithiol, (c) 1,3-propanedithiol, (d) 1,4-butanedithiol, (e) 1,6-hexanedithiol, (f) 1,8-octanedithiol, (g) 1,9-nonanedithiol, (h) 1,3-diiodopropane, (i) 1,8-dichlorooctane, (j) 1,8-dibromooctane, and (k) 1,8-diiodooctane.

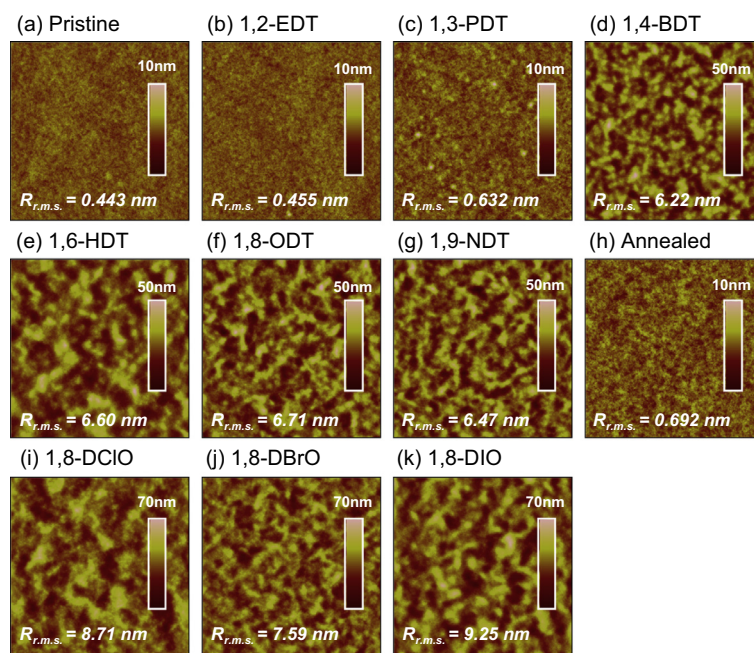


Fig. 6. AFM topographies of films cast from **P3HT:PC₆₁BM**: (a) without additives; with the additives (b) 1,2-ethanedithiol, (c) 1,3-propanedithiol, (d) 1,4-butanedithiol, (e) 1,6-hexanedithiol, (f) 1,8-octanedithiol, (g) 1,9-nonanedithiol, (i) 1,8-dichlorooctane, (j) 1,8-dibromooctane, (k) 1,8-diiodooctane; (h) annealed at 150 °C without processing additives.

Table 1 shows the characteristics of the photovoltaic devices based on **PONTBT:PC₇₁BM** with processing additives, namely current density (J_{SC}), open circuit voltage (V_{OC}), fill

factor (FF), and PCE. The cell based on **PONTBT:PC₇₁BM** incorporating 2 vol% of 1,2-EDT exhibits the best PCE (5%) of the blends processed with additives with various alkyl

chain lengths. The cell based on **PONTBT**:PC₇₁BM incorporating 2 vol% of 1,8-DIO exhibits the highest PCE (4.5%) of the octane blends processed with additives with various end-group electronegativities. 1,8-DIO has the end group with the lowest electronegativity of the processing additives from 1,8-DCIO to 1,8-DIO (Fig. S6(b)).

However, the cell based on **PONTBT**:PC₇₁BM incorporating 2 vol% of 1,3-diiodopropane (1,3-DIP) exhibits an even better PCE (5.5%), as well as an enhanced J_{SC} and the highest FF value (Table 1 and Fig. 7(a)). Note that 1,2-diiodoethane (1,2-DIE) does not dissolve in dichlorobenzene, therefore 1,3-DIP was used instead of 1,2-DIE. Thus the solubility of PC₇₁BM in processing additives with sufficiently short alkyl chains or end groups with sufficiently low electronegativity induces adequate phase separation of **PONTBT** in **PONTBT**:PC₇₁BM cells.

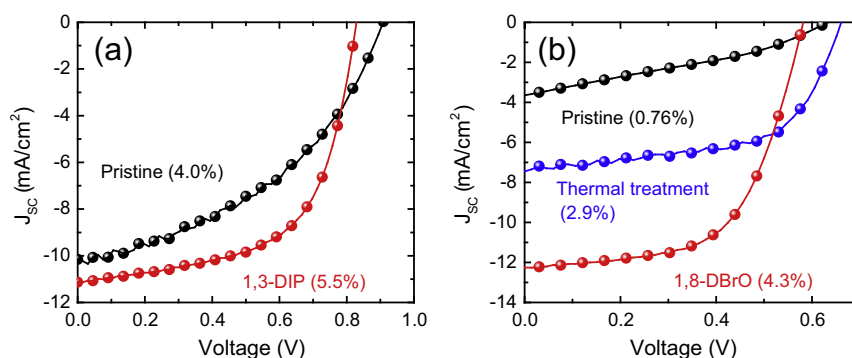


Fig. 7. The J - V curves of photovoltaic devices based on (a) **PONTBT**:PC₇₁BM (1:3, w/w) and (b) **P3HT**:PC₆₁BM (1:1, w/w) with or without 2% processing additive under AM 1.5G illumination at an intensity of 100 mW/cm².

Table 1

Performances of OPVs^a based on **PONTBT**:PC₇₁BM and **P3HT**:PC₆₁BM under AM 1.5G illumination at an intensity of 100 mW/cm².

Electron donor	Alkyl length ^b	End group ^{c,d}	V_{OC} (V)	J_{SC} (mA/cm ²)	FF (%)	PCE (%)	
PONTBT	w/o ^e	-SH	0.91 ± 0.01	10.2 ± 0.7	43.3 ± 1.5	4.0 ± 0.49	
	Ethane	-SH	0.83 ± 0.01	13.9 ± 0.3	43.1 ± 1.3	5.0 ± 0.30	
	Propane	-SH	0.85 ± 0.01	12.6 ± 0.3	42.9 ± 1.0	4.6 ± 0.27	
	Butane	-SH	0.80 ± 0.01	12.7 ± 0.2	37.8 ± 1.1	3.8 ± 0.26	
	Hexane	-SH	0.82 ± 0.01	12.0 ± 0.5	33.8 ± 1.5	3.3 ± 0.36	
	Octane	-SH	0.82 ± 0.01	11.6 ± 0.8	31.9 ± 2.0	3.0 ± 0.49	
	Nonane	-SH	0.82 ± 0.02	7.2 ± 2.4	21.7 ± 4.0	1.3 ± 0.77	
	Octane	-Cl	0.80 ± 0.02	11.2 ± 1.2	29.5 ± 3.0	2.6 ± 0.70	
	Octane	-Br	0.79 ± 0.01	13.5 ± 0.6	39.2 ± 2.5	4.2 ± 0.50	
	Octane	-I	0.82 ± 0.01	11.8 ± 0.3	46.9 ± 2.0	4.5 ± 0.41	
	Propane	-I	0.83 ± 0.01	11.1 ± 0.2	59.8 ± 1.2	5.5 ± 0.29	
	P3HT	w/o	-SH	0.64 ± 0.02	3.6 ± 0.7	32.7 ± 4.4	0.76 ± 0.29
		Annealing ^f	-SH	0.67 ± 0.01	7.4 ± 0.2	58.5 ± 1.9	2.9 ± 0.22
Ethane		-SH	0.71 ± 0.01	3.8 ± 0.4	35.4 ± 2.3	0.96 ± 0.18	
Butane		-SH	0.59 ± 0.01	9.5 ± 0.5	42.2 ± 1.7	2.4 ± 0.23	
Hexane		-SH	0.59 ± 0.01	10.4 ± 0.4	52.2 ± 1.5	3.2 ± 0.28	
Nonane		-SH	0.58 ± 0.02	12.2 ± 0.2	52.3 ± 1.2	3.7 ± 0.28	
Octane		-Cl	0.55 ± 0.02	12.3 ± 0.2	50.7 ± 2.4	3.4 ± 0.38	
Octane		-Br	0.58 ± 0.01	12.3 ± 0.2	60.2 ± 2.1	4.2 ± 0.39	
Octane		-I	0.58 ± 0.01	11.0 ± 0.3	52.6 ± 3.1	3.3 ± 0.41	

^a The data shown are the average values obtained from 20 devices with standard deviation.

^b The alkyl length of processing additives based on alkanedithiols or alkanedihaliides.

^c The functional end group of processing additives based on alkanedithiols or alkanedihaliides.

^d SH: -dithiol, -Cl: dichloro-, -Br: dibromo-, and -I: diiodo-.

^e These films were fabricated without processing additives and thermal annealing process.

^f These films fabricated without processing additives were annealed at 150 °C for 20 min in a N₂ glove box.

Table 1 and Fig. 8 summarize the V_{OC} , J_{SC} , FF, and PCE values of the devices based on **PONTBT**:PC₇₁BM (1:3) blends. The V_{OC} values are in the range 0.79–0.85 V and are insensitive to variation of the processing additive, whereas the J_{SC} , FF, and PCE values are sensitive to this variation. For the **P3HT**:PC₆₁BM cells, as the lengths of the alkyl chains in the processing additives increase, the J_{SC} , FF, and PCE values increase (Fig. S6 and Table 1).

Fig. 7(b) and S7 displays the J - V curves for devices based on **P3HT**:PC₆₁BM with processing additives possessed end groups with various electronegativities. The best device performance was obtained with a **P3HT**:PC₆₁BM blend with 2 vol% of 1,8-DBrO (Table 1). For the **P3HT**:PC₆₁BM cells, the processing additives with long alkyl chains or strongly electronegative end groups increase the crystallinity of **P3HT**.

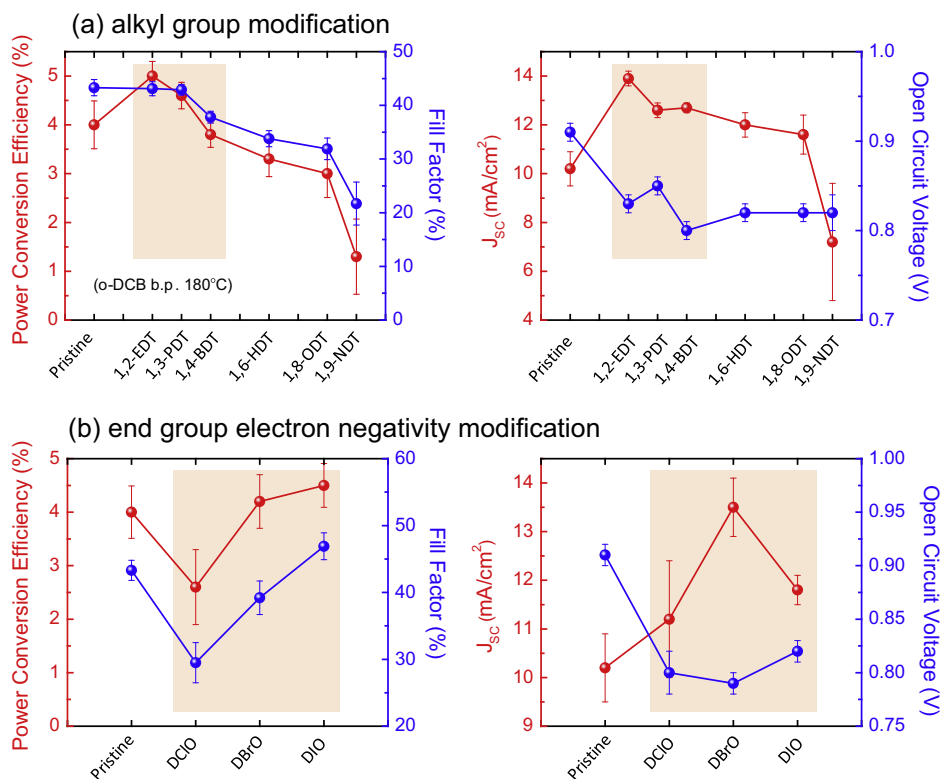


Fig. 8. Summary of the photovoltaic performances of cells based on **PONTBT**:PC₇₁BM (1:3, w/w) with or without 2% processing additives (a) with various alkyl chain lengths and (b) with end groups with various electronegativities under AM 1.5G illumination at an intensity of 100 mW/cm².

For the **PONTBT**:PC₇₁BM blends, the optimum morphologies are obtained by incorporating processing additives with short alkyl chains or end groups with low electronegativities. In contrast, the photovoltaic performances of the **P3HT**:PC₆₁BM cells are improved by incorporating processing additives with long alkyl chains or strongly electronegative end groups.

4. Conclusions

We have studied the development of the bulk heterojunction morphologies of conjugated polymer/fullerene derivative blends in the presence of processing additives; **PONTBT** and **P3HT** were used as conjugated polymers. UV-visible spectra show that the intermolecular interactions between the two polymers and the processing additives vary with their alkyl chain lengths and the electronegativities of their end groups. Cells based on a **PONTBT**:PC₇₁BM blend incorporating 2 vol% of 1,3-DIP, which has short alkyl chains and end group with lower electronegativity exhibit the best performance, in particular enhanced J_{sc} and FF values. The phase separation of the **PONTBT** phase and the PC₇₁BM phase increases for **PONTBT**:PC₇₁BM blends incorporating longer alkyl chain and high electronegative end group processing additives. For the **P3HT**:PC₆₁BM blend, processing additives with longer alkyl chains and strongly electronegative end groups

enhance the π - π coupling of P3HT, which enhances J_{sc} . The incorporation of the additive 1,8-DBrO was found to produce the highest PCE in the **P3HT**:PC₆₁BM cells.

Acknowledgements

This work was supported by the National Research Foundation of South Korea (NRF) grant funded by the Korea government (MSIP) (2012R1A2A2A06047047) and the Center for Advanced Soft Electronics under the Global Frontier Research Program (Nos. 20110031639 & 2013M3A6A5073172) through the National Research Foundation funded by the Ministry of Education, Science and Technology (Korea).

Appendix A. Supplementary material

Supplementary data associated with this article can be found, in the online version, at <http://dx.doi.org/10.1016/j.orgel.2014.10.006>.

References

- [1] R.F. Service, Outlook brightens for plastic solar cells, *Science* 332 (2011) 293.
- [2] M.A. Green, K. Emery, Y. Hishikawa, W. Warta, Progress in photovoltaics: research and applications, *Prog. Photovoltaics* 19 (2011) 84–92.

- [3] H.-Y. Chen, J. Hou, S. Zhang, Y. Liang, G. Yang, Y. Yang, L. Yu, Y. Wu, G. Li, Polymer solar cells with enhanced open-circuit voltage and efficiency, *Nat. Photon.* 3 (2009) 649–653.
- [4] Z. He, C. Zhong, X. Huang, W.-Y. Wong, H. Wu, L. Chen, S. Su, Y. Cao, Simultaneous enhancement of open-circuit voltage, short-circuit current density, and fill factor in polymer solar cells, *Adv. Mater.* 23 (2011) 4636–4643.
- [5] L. Dou, J. You, J. Yang, C.-C. Chen, Y. He, S. Murase, T. Moriarty, K. Emery, G. Li, Y. Yang, Tandem polymer solar cells featuring a spectrally matched low-bandgap polymer, *Nat. Photon.* 6 (2012) 180–185.
- [6] B. Walker, C. Kim, T.-Q. Nguyen, Small molecule solution-processed bulk heterojunction solar cells, *Chem. Mater.* 23 (2011) 470–482.
- [7] Z. He, C. Zhong, S. Su, M. Xu, H. Wu, Y. Cao, Enhanced power-conversion efficiency in polymer solar cells using an inverted device structure, *Nat. Photonics* 6 (2012) 591–595.
- [8] A.K.K. Kyaw, D.H. Wang, D. Wynands, J. Zhang, T.-Q. Nguyen, G.C. Bazan, A.J. Heeger, Improved light harvesting and improved efficiency by insertion of an optical spacer (zno) in solution-processed small-molecule solar cells, *Nano Lett.* 13 (2013) 3796–3801.
- [9] J. You, L. Dou, K. Yoshimura, T. Kato, K. Ohya, T. Moriarty, K. Emery, C.C. Chen, J. Gao, G. Li, Y. Yang, A polymer tandem solar cell with 10.6% power conversion efficiency, *Nat. Commun.* 4 (2013) 1446–1455.
- [10] J. You, C.-C. Chen, Z. Hong, K. Yoshimura, K. Ohya, R. Xu, S. Ye, J. Gao, G. Li, Y. Yang, 10.2% Power conversion efficiency polymer tandem solar cells consisting of two identical sub-cells, *Adv. Mater.* 25 (2013) 3973–3978.
- [11] D. Credgington, R. Hamilton, P. Atienzar, J. Nelson, J.R. Durrant, Non-geminate recombination as the primary determinant of open-circuit voltage in polythiophene:fullerene blend solar cells: an analysis of the influence of device processing conditions, *Adv. Funct. Mater.* 21 (2011) 2744–2753.
- [12] P.E. Keivanidis, V. Kamm, W. Zhang, G. Floudas, F. Laquai, I. McCulloch, D.D.C. Bradley, J. Nelson, Correlating emissive non-geminate charge recombination with photocurrent generation efficiency in polymer/perylene diimide organic photovoltaic blend films, *Adv. Funct. Mater.* 22 (2012) 2318–2326.
- [13] H. Mangold, A.A. Bakulin, I.A. Howard, C. Kästner, D.A.M. Egbe, H. Hoppe, F. Laquai, Control of charge generation and recombination in ternary polymer/polymer:fullerene photovoltaic blends using amorphous and semi-crystalline copolymers as donors, *Phys. Chem. Chem. Phys.* (2014), <http://dx.doi.org/10.1039/c4cp01883d>.
- [14] C.J. Schaffer, C.M. Palumbino, M.A. Niedermeier, C. Jendrzewski, G. Santoro, S.V. Roth, P. Müller-Buschbaum, A direct evidence of morphological degradation on a nanometer scale in polymer solar cells, *Adv. Mater.* 25 (2013) 6760–6764.
- [15] O.V. Mikhnenko, H. Azimi, M. Scharber, M. Morana, P.W.M. Blom, M.A. Loi, Exciton diffusion length in narrow bandgap polymers, *Energy Environ. Sci.* 5 (2012) 6960–6965.
- [16] W.A. Luhman, R.J. Holmes, Investigation of energy transfer in organic photovoltaic cells and impact on exciton diffusion length measurements, *Adv. Funct. Mater.* 21 (2011) 764–771.
- [17] E. Zhou, J. Cong, K. Hashimoto, K. Tajima, Control of miscibility and aggregation via the material design and coating process for high-performance polymer blend solar cells, 25 (2013) 6991–6996.
- [18] J.R. Tumbleston, B.A. Collins, L. Yang, A.C. Stuart, E. Gann, W. Ma, W. You, H. Ade, The influence of molecular orientation on organic bulk heterojunction solar cells, *Nat. Photon.* 8 (2014) 385–391.
- [19] Z. Xu, L.-M. Chen, G. Yang, C.-H. Huang, J. Hou, Y. Wu, G. Li, C.-S. Hsu, Y. Yang, Vertical phase separation in poly(3-hexylthiophene):fullerene derivative blends and its advantage for inverted structure solar cells, *Adv. Funct. Mater.* 19 (2009) 1227–1234.
- [20] G. Li, V. Shrotriya, J. Huang, Y. Yao, T. Moriarty, K. Emery, Y. Yang, High-efficiency solution processable polymer photovoltaic cells by self-organization of polymer blends, *Nat. Mater.* 4 (2005) 864–868.
- [21] J.H. Park, J.S. Kim, J.H. Lee, W.H. Lee, K. Cho, Effect of annealing solvent solubility on the performance of poly(3-hexylthiophene)/methanofullerene solar cells, *J. Phys. Chem. C* 113 (2009) 17579–17584.
- [22] F. Padinger, R.S. Rittberger, N.S. Sariciftci, Effects of postproduction treatment on plastic solar cells, *Adv. Funct. Mater.* 13 (2003) 85–88.
- [23] C.R. McNeill, J.J.M. Halls, R. Wilson, G.L. Whiting, S. Berkebile, M.G. Ramsey, R.H. Friend, N.C. Greenham, Efficient polythiophene/polyfluorene copolymer bulk heterojunction photovoltaic devices: device physics and annealing effects, *Adv. Funct. Mater.* 18 (2008) 2309–2321.
- [24] S.H. Park, A. Roy, S. Beaupre, S. Cho, N. Coates, J.S. Moon, D. Moses, M. Leclerc, K. Lee, A.J. Heeger, Bulk heterojunction solar cells with internal quantum efficiency approaching 100%, *Nat. Photon.* 3 (2009) 297–302.
- [25] C.W. Rochester, S.A. Mauger, A.J. Moulé, Investigating the morphology of polymer/fullerene layers coated using orthogonal solvents, *J. Phys. Chem. C* 116 (2012) 7287–7292.
- [26] Y. Liang, Z. Xu, J. Xia, S.-T. Tsai, Y. Wu, G. Li, C. Ray, L. Yu, For the bright future-bulk heterojunction polymer solar cells with power conversion efficiency of 7.4%, *Adv. Mater.* 22 (2010) E135–E138.
- [27] H.-Y. Chen, J. Hou, S. Zhang, Y. Liang, G. Yang, Y. Yang, L. Yu, Y. Wu, G. Li, Efficiency enhancement in low-bandgap polymer solar cells by processing with alkane dithiols, *Nat. Mater.* 6 (2007) 497–500.
- [28] S.-H. Jin, B.V.K. Naidu, H.-S. Jeon, S.-M. Park, J.-S. Park, S.C. Kim, J.W. Lee, Y.-S. Gal, Priority publishing in solar energy materials and solar cells, *Sol. Energy Mater. Sol. Cells* 94 (2010) 1187–1190.
- [29] M.T. Dang, G. Wantz, H. Bejoubji, M. Urien, O.J. Dautel, L. Vignau, L. Hirsch, Polymeric solar cells based on p3ht:pcbm: role of the casting solvent, *Sol. Energy Mater. Sol. Cells* 95 (2011), 3408–3408.
- [30] T.K. An, I. Kang, H.-J. Yun, H. Cha, J. Hwang, S. Park, J. Kim, Y.J. Kim, D.S. Chung, S.-K. Kwon, Y.-H. Kim, C.E. Park, Solvent additive to achieve highly ordered nanostructural semicrystalline dpp copolymers: toward a high charge carrier mobility, *Adv. Mater.* 25 (2013) 7003–7009.
- [31] T.K. An, S.-M. Park, S. Nam, J. Hwang, S.-J. Yoo, M.-J. Lee, W.M. Yun, J. Jang, H. Cha, J. Hwang, S. Park, J. Kim, D.S. Chung, Y.-H. Kim, S.-K. Kwon, C.E. Park, Thin film morphology control via a mixed solvent system for high-performance organic thin film transistors, *Sci. Adv. Mater.* 5 (2013) 1323–1327.
- [32] J. Peet, J.Y. Kim, N.E. Coates, W.L. Ma, D. Moses, A.J. Heeger, G.C. Bazan, Efficiency enhancement in low-bandgap polymer solar cells by processing with alkane dithiols, *Nat. Mater.* 6 (2007) 497–500.
- [33] J. Peet, C. Soci, R.C. Coffin, T.Q. Nguyen, A. Mikhailovsky, D. Moses, G.C. Bazan, Method for increasing the photoconductive response in conjugated polymer/fullerene composites, *Appl. Phys. Lett.* 89 (2006), 252105-3.
- [34] J.K. Lee, W.L. Ma, C.J. Brabec, J. Yuen, J.S. Moon, J.Y. Kim, K. Lee, G.C. Bazan, A.J. Heeger, Processing additives for improved efficiency from bulk heterojunction solar cells, *J. Am. Chem. Soc.* 130 (2008) 3619–3623.
- [35] F. Etzold, I.A. Howard, N. Forler, D.M. Cho, M. Meister, H. Mangold, J. Shu, M.R. Hansen, K. Müllen, F. Laquai, The effect of solvent additives on morphology and excited-state dynamics in pcpdttb:pcbm photovoltaic blends, *J. Am. Chem. Soc.* 134 (2012) 10569–10583.
- [36] Y. Liang, D. Feng, Y. Wu, S.-T. Tsai, G. Li, C. Ray, L. Yu, Highly efficient solar cell polymers developed via fine-tuning of structural and electronic properties, *J. Am. Chem. Soc.* 131 (2009) 7792–7799.
- [37] T.-Y. Chu, S.-W. Tsang, J. Zhou, P.G. Verly, J. Lu, S. Beaupré, M. Leclerc, Y. Tao, High-efficiency inverted solar cells based on a low bandgap polymer with excellent air stability, *Sol. Energy Mater. Sol. Cells* 96 (2012) 155–159.
- [38] T. Chu, J. Lu, S. Beaupré, Y. Zhang, J.-R. Pouliot, S. Wakim, J. Zhou, M. Leclerc, Z. Li, J. Ding, Y. Tao, Bulk heterojunction solar cells using thieno [3,4-c]pyrrole-4,6-dione and dithieno[3,2-b:2',3'-d]silole copolymer with a power conversion efficiency of 7.3%, *J. Am. Chem. Soc.* 133 (2011) 4250–4253.
- [39] T. Salim, L.H. Wong, B. Bräuer, R. Kukreja, Y.L. Foo, Z. Bao, Y.M. Lam, Solvent additives and their effects on blend morphologies of bulk heterojunctions, *J. Mater. Chem.* 21 (2011) 242–250.
- [40] J. Ouyang, Y. Xia, High-performance polymer photovoltaic cells with thick p3ht:pcbm films prepared by a quick drying process, *Sol. Energy Mater. Sol. Cells* 93 (2009) 1592–1597.
- [41] Y. Yao, J. Hou, Z. Xu, G. Li, Y. Yang, Effects of solvent mixtures on the nanoscale phase separation in polymer solar cells, *Adv. Funct. Mater.* 18 (2008) 1783–1789.
- [42] H.-Y. Chen, H. Yang, G. Yang, S. Sista, R. Zadoyan, G. Li, Y. Yang, Fast-grown interpenetrating network in poly(3-hexylthiophene):methanofullerenes solar cells processed with additive, *J. Phys. Chem. C* 113 (2009) 7946–7953.
- [43] S.-O. Kim, D.S. Chung, H. Cha, M.C. Hwang, J.-W. Park, Y.-H. Kim, C.E. Park, S.-K. Kwon, Efficient polymer solar cells based on dialkoxynaphthalene and benzo[c][1,2,5]thiadiazole: a new approach for simple donor–acceptor pair, *Sol. Energy Mater. Sol. Cells* 95 (2011) 1678–1685.

- [44] J.Y. Kim, S.H. Kim, H.-H. Lee, K. Lee, W. Ma, X. Gong, A.J. Heeger, New architecture for high-efficiency polymer photovoltaic cells using solution-based titanium oxide as an optical spacer, *Adv. Mater.* 18 (2006) 572–576.
- [45] W. Ma, C. Yang, X. Gong, K. Lee, A.J. Heeger, Thermally stable, efficient polymer solar cells with nanoscale control of the interpenetrating network morphology, *Adv. Funct. Mater.* 15 (2005) 1617–1622.
- [46] S. Yum, T.K. An, X. Wang, W. Lee, M.A. Uddin, Y.J. Kim, T.L. Nguyen, S. Xu, S. Hwang, C.E. Park, H.Y. Woo, Benzotriazole-containing planar conjugated polymers with noncovalent conformational locks for thermally stable and efficient polymer field-effect transistors, *Chem. Mater.* 26 (26) (2014) 2147–2154.